

# Multipolar planetary nebulae: Not as geometrically diversified as thought

Sze-Ning Chong<sup>1</sup>, Sun Kwok<sup>2</sup>, Hiroshi Imai<sup>1</sup>, and Daniel Tafoya<sup>1</sup>

<sup>1</sup>Graduate School of Science and Engineering,  
Kagoshima University, 1-21-35 Korimoto,  
Kagoshima 890-0065, Japan

email: selina@milkyway.sci.kagoshima-u.ac.jp

<sup>2</sup>Department of Physics, The University of Hong Kong  
Pokfulam Road, Hong Kong  
email: sunkwok@hku.hk

**Abstract.** We present a general three-dimensional model of multipolar planetary nebulae (PNe). By rotating to different viewing angles and adjusting the angles between the multiple lobes, we demonstrate that the model is able to reproduce HST H $\alpha$  images of 20 multipolar young PNe. Though this model only considers the geometrical projection effects, it significantly unifies the selected PNe and can be considered as a first-order fundamental model of the “multipolar” morphological class. This kind of model reduces complexity and is essential to pursuing of the shaping mechanism. In addition, we illustrate that under some special conditions, i.e. in certain viewing angles, or with low sensitivity, it will be hard to imagine that the projected image originates from a multipolar-lobed model.

**Keywords.** (ISM:) planetary nebulae: general

---

## 1. Introduction

As the telescope power improves, more multipolar PNe have been discovered, and more known bipolar PNe have been or are ready to be re-classified as multipolar, e.g. NGC 2440 (Wang et al. 2008), NGC 6072 (Kwok et al. 2010) and NGC 6853 (Kwok et al. 2008). Multipolar structures make the game more challenging: while the formation mechanisms of bipolar PNe remain unclear, in order to explain the presence of multiple outflow axes one has to introduce additional hypotheses such as precession motions (Yung et al., this volume). It is still under debate whether the multiple lobes are formed simultaneously or episodically (Sahai 2002). They may involve totally different physical processes.

Before starting to establish the theories, the first step should be to know the real three-dimensional (3D) structure, rather than only the projected two-dimensional (2D) images of these PNe. Based on the 3D model, one can estimate the kinematic timescale in each outflow direction to verify whether they were produced at the same time. Instead of making a single model for each nebula, it will be more effective if we can build a unified 3D model to reproduce the observed 2D images of individual objects by changing only a few parameters. Similarities and differences can then be more easily seen from the varying parameters.

## 2. The Model

We used SHAPE (Steffen 2011) to construct the 3D model. Basically, the model consists of three pairs of identical lobes. At the moment, we are concerned about the projection effect on the lobes in different orientations, so we fix other parameters such as the sizes, and change only the inclination angle  $i$  and position angle (PA) of each pair. Therefore

there are six independent parameters. From these six parameters, the separation angle  $\theta$  between any two pairs of lobes can be calculated from the inner product. The lobes are hollow inside with evenly distributed density within the “walls” of the lobes. The brightness is proportional to the square of the column density.



**Figure 1.** Perception of morphology is affected by viewing angle and sensitivity. *Upper row:* With the six angles in the model fixed, the viewing angle is changed from each image to the next by  $15^\circ$  of  $i$  and  $15^\circ$  of PA. *Lower row:* Each image is modified from the one above that the faintest pixels below one-third of the peak brightness are cut off. Brightness levels are shown in linear scale.

Fig. 1 (upper row) shows the projection effect on a particular model rotated to different viewing angles. Although the true sizes of lobes are the same, the apparent length changes with the viewing angle. In some special cases, the projected image may not reveal its real multipolar structure (Fig. 2). For examples, this happens when projections or two or more pairs of lobes are aligned along the same direction. If one pair is viewed nearly pole-on or slightly tilted in the equatorial direction, it may be wrongly interpreted as a torus.



**Figure 2.** Some special combinations of the six angles make the projected images not easily interpreted as multipolar morphologies. Brightness levels are shown in log scale.

In addition, sensitivity has to be taken into account. Fig. 1 illustrates a comparison between the images under high and low sensitivity conditions. If the faint outer parts are filtered out due to low sensitivity, it will be hard to see that the PN is multipolar.

### 3. Results and Discussions

#### 3.1. Comparison with Observations

To compare the modeled images with real observed ones, we searched through the literatures (Sahai et al. 2011, Ueta et al. 2007, Guerrero et al. 2008, Harman et al. 2004, and references therein) for suitable objects which have been observed in  $H\alpha$  with the Wide-Field Planetary Camera 2 (WFPC2) of the Hubble Space Telescope (HST). The sample contains a total of 20 PNe images retrieved from the Canadian Astronomy Data Center (CADDC) archive (details are listed in Table 1). We do not claim that the sample is representative of all multipolar PNe; we hope to demonstrate that our model can be the first-order solutions to the true morphologies of the selected objects.

For simplicity, we change only the six angles as described in the previous section and keep all other things unchanged. The results are presented in Fig. 3 and Table 1.

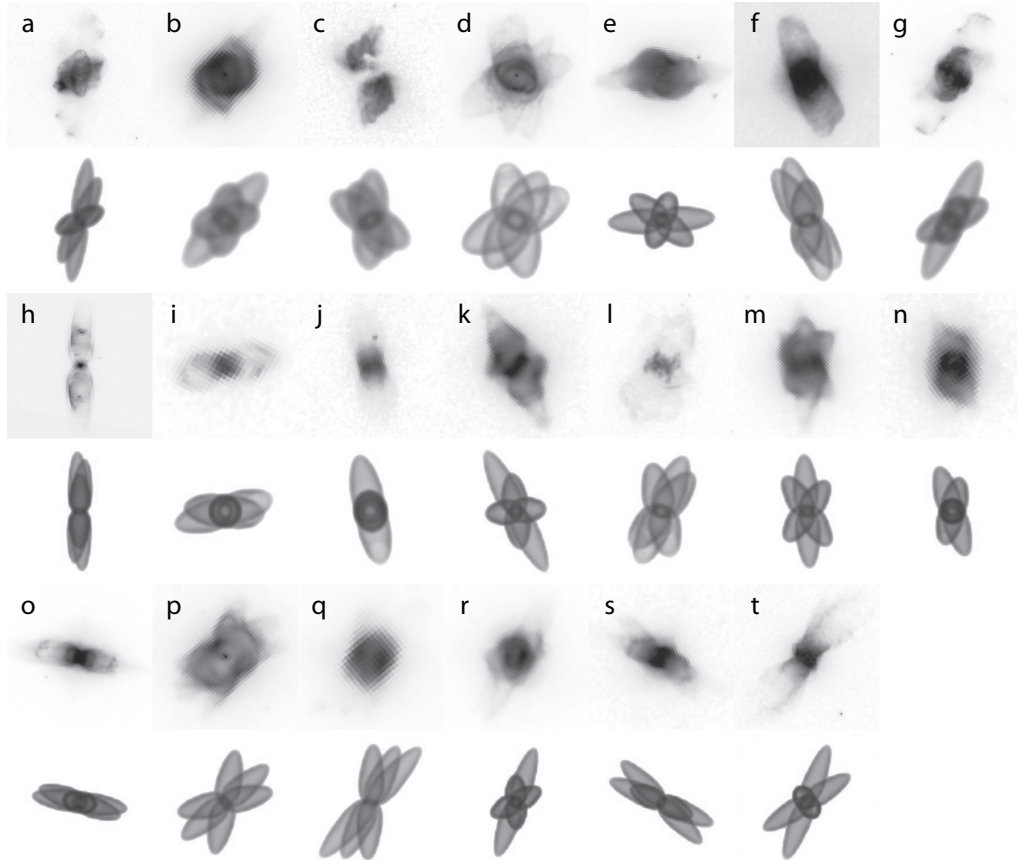


**Figure 3.** Comparison of the 20 observed images (those with an index letter) with its corresponding modeled image (the one right below it). Brightness levels are in log scale. North is pointing up and east to the left. Refer to Table 1 for the object data. The angular sizes and brightness levels of the objects are not the same.

### 3.2. Why We Choose the Number 3

In general, “multipolar” means having more than one pair of lobes, not confined to three pairs. For the objects chosen, at least three pairs are obviously seen, and the number 3 is also commonly found in literatures (NGC 7027 by Nakashima et al. 2010; NGC 6644 by Hsia et al. 2010; and NGC 7026 by Clark et al., this volume). It is possible that there are more than three pairs (for example, IRAS 19024+0044 by Sahai et al. 2005; and NGC 5189 by Sabin et al., this volume), but adding more pairs means adding more parameters; at this stage we hope to keep the number of parameters down. The less obvious lobes can be treated as higher ordered structures.

### 3.3. Lobes: Same Length or Not?

By looking at a 2D image, it is hard to tell whether the lobes have the same length or not without knowing the inclination angle. Kinematic information are needed to determine the actual length ratios. Lobes with same lengths are likely to be produced simultaneously with the same outflow velocities. In this case, the ratios of the velocity components along the line-of-sight should be able to tell the projected angles independently. On the other hand, for lobes of different lengths the true length ratios are more uncertain.

**Table 1.** Information and parameters of the 20 PNe. The order of pairs 1, 2 and 3 is arbitrary.  $i$  is the inclination angle between the elongated direction of a pair of lobes and the line-of-sight;  $\theta$  (minimum, median or maximum) refer to the separation angles between pairs.

	IRAS Name	Dataset	Pair 1		Pair 2		Pair 3		$\theta^\circ$		
			$i^\circ$	PA $^\circ$	$i^\circ$	PA $^\circ$	$i^\circ$	PA $^\circ$	min	med	max
a	05028+1038	U39H1301B	90	48	22	8	25	64	33.1	44.8	77.9
b	07172-2138	U5HH0502B	16	17	33	75	10	41	17.6	20.0	21.7
c	10197-5750	U3B30201B	26	20	23	2	-24	-57	12.0	12.0	23.7
d	10214-6017	U35T1407B	22	23	21	-11	62	30	12.1	14.6	26.3
e	15015-5459	U35T2905B	37	17	21	87	21	-40	19.0	33.5	51.7
f	16409-1851	U5HH3102B	20	36	32	0	-17	-33	9.8	18.0	18.7
g	16585-2145	U47B0201B	48	25	14	25	63	25	16.0	31.2	33.4
h	17028-1004	U42I0202B	30	55	45	0	-2	6	11.7	15.5	25.1
i	17156-3135	U6MG5001B	20	27	0	-85	74	0	11.0	20.1	27.1
j	17296-3641	U6MG4801B	3	31	6	-18	-12	-9	3.0	24.5	27.4
k	17389-2409	U6MG1501B	50	18	24	-26	84	-7	28.2	29.6	46.2
l	17410-3405	U6MG3101B	25	32	25	40	23	-12	10.5	17.7	21.6
m	17496-2221	U5HH6902B	40	23	27	-3	35	-33	20.6	25.7	27.3
n	17549-3347	U6MG3601B	0	31	22	0	-18	14	16.6	21.6	31.2
o	17567-3849	U5HH1302B	41	35	10	-82	-71	-79	8.5	25.1	30.3
p	18022-2822	U35T2105B	37	39	33	12	50	77	17.5	23.3	36.1
q	18039-2913	U5HH4103B	41	45	58	3	26	42	16.0	18.4	34.0
r	18430-1430	U59B0301B	21	52	20	62	19	0	20.5	33.2	38.4
s	19431+2112	U59B0704B	51	50	27	-44	-67	-65	17.8	23.5	27.7
t	20090+3715	U39H3601B	15	52	90	-43	61	23	51.5	57.3	84.0

#### 4. Further Studies

It is unclear why the separation angles vary from a PN to the other. The model introduced here provides the stage for further developments. The chemical abundances and spectral energy distributions (SEDs) are properties to be studied in the next step. Furthermore, changing density profiles, adding other components, radiative transfer treatments, and interaction with the interstellar medium are examples of some of the potential simulations. The 20 PNe presented is barely the tip of the iceberg among the known multipolar PNe, and it can be expected that total number will keep increasing.

The work was supported by a grant awarded to SK from the Research Grants Council of the Hong Kong Special Administrative Region, China (Project No. HKU 7031/10P).

#### References

- Guerrero, M., Miranda, L.F., Riera, A., Velázquez, P.F., Olgúin, L., Vázquez, R., Chu, Y.-H., Raga, A., & Benítez, G. 2008, *ApJ*, 683, 272
- Harman, D.J., Bryce, M., López, J.A., Meaburn, J., & Holloway, A.J. 2004, *MNRAS*, 348, 1047
- Hsia, C.-H., Kwok, S., Zhang, Y., Koning, N., & Volk, K. 2010, *ApJ*, 725, 173
- Kwok, S., Chong, S.-N., Koning, N., Hua, T., & Yan, C.-Y. 2008, *ApJ*, 689, 219
- Kwok, S., Chong, S.-N., Hsia, C.-H., Zhang, Y., & Koning, N. 2010, *ApJ*, 708, 93
- Nakashima, J., Kwok, S., Zhang, Y., & Koning, N. 2010, *AJ*, 140, 490
- Ratag, M.A., Pottasch, S.R., Dennefeld, M., & Menzies, J. 1997, *A&AS*, 126, 297
- Sahai, R. 2002, *Rev. Mexicana AyA*, 13, 133
- Sahai, R., Sánchez Contreras, C., & Morris, M. 2005, *ApJ*, 620, 948
- Sahai, R., Morris, M.R., & Villar, G.G. 2011, *AJ*, 141, 134
- Steffen, W. 2011, *IEEE TVCG*, vol. 17, no.4, pp.454
- Ueta, T., Murakawa, K., & Meixner, M. 2007, *AJ*, 133, 1345
- Wang, M.-Y., Hasegawa, T.I., & Kwok, S. 2008, *ApJ*, 673, 264